# Structural and Thermotropic Properties of Calcium-Dimyristoylphosphatidic Acid Complexes at Acidic and Neutral pH Conditions

Hiroshi Takahashi,* Takashi Yasue,* Kazuo Ohki,‡ and Ichiro Hatta*

*Department of Applied Physics, School of Engineering, Nagoya University, Nagoya 464–01, and ‡Department of Physics, Faculty of Science, Tohoku University, Sendai 980, Japan

ABSTRACT   Two kinds of calcium-dimyristoylphosphatidic acid (DMPA) complexes at acidic and neutral pH conditions were prepared in the following ways. The complex at pH 4 was obtained by adding $Ca^{2+}$ to DMPA dispersion in pure water. On the other hand, the complex at pH 7.4 was obtained by adding $Ca^{2+}$ to DMPA dispersion in the presence of NaOH. The stoichiometries of $Ca^{2+}$ ion to DMPA molecule are 0.5–0.67 and ~1 for the complexes at pH 4 and 7.4, respectively. Static x-ray diffraction shows that the hydrocarbon chains of the $Ca^{2+}$-DMPA complex at pH 4 at 20°C are more tightly packed than those of the complex at pH 7.4 at 20°C. Furthermore, the complex at pH 4 at 20°C gives rise to several reflections that might be related to the ordered arrangement of the $Ca^{2+}$ ions. These results indicate that the structure of the complex at pH 4 is crystalline-like. In the differential scanning calorimetry (DSC) thermogram, the complex at pH 7.4 undergoes no phase transition in a temperature range between 30 and 80°C. On the other hand, in the DSC thermogram for the complex at pH 4, a peak appears at 65.8°C in the first heating scan. In the successive second heating scan, a transition peak appears at 63.5°C. In connection with the DSC results, the structural changes associated with these phase transitions were studied with temperature-scan x-ray diffraction. In the first heating scan, although a peak appears at 65.8°C in the DSC thermogram, the hydrocarbon chain packing gradually converts from an orthorhombic lattice to a hexagonal lattice near 52°C, and successively the chain melting phase transition occurs near 67°C. In the second heating scan, the hydrocarbon chains are packed in a hexagonal lattice over the whole temperature range and the chain melting phase transition occurs near 63.5°C. Therefore, the $Ca^{2+}$-DMPA complex at pH 4 has a metastable state. The metastable state transforms to a stable state by maintaining the complex at pH 4 for about 90 h at 20°C.

## INTRODUCTION

Although usually a small amount of phosphatidic acid (PA) is found in biomembranes, this lipid is believed to play a number of important roles in biological function. Furthermore, PA is a key intermediate in the biosynthesis of glycerophospholipids. In recent years, it has been made clear that PA is indirectly associated with the activation of protein kinase C (Nishizuka, 1992; Dennis et al., 1991). In addition, it has been pointed out that PA behaves as an ionophor for calcium ions (Ohki et al., 1986; Smaal et al., 1987), and as a result, PA works in the adjustment function of calcium concentration in a cell. Therefore, it is of interest to clarify the nature of the interaction between PA and calcium ions. Thus, many studies on the interaction between PA and calcium ions have already been carried out. For example, it is well known that calcium ions induce lateral phase separation in mixed lipid systems, including PA (Graham et al., 1985; Kouaouci et al., 1985; Eklund et al., 1988; Ohki, 1988; Ohki et al., 1989). Besides these studies, the effects of $Ca^{2+}$ ions on the structural and thermotropic properties of a PA bilayer have been studied. At physiolog-

ical pH, in the temperature range between 10 and 100°C, no gel-to-liquid crystalline phase transition has been observed for $Ca^{2+}$-dimyristoylphosphatidic acid (DMPA) and $Ca^{2+}$-dipalmitoylphosphatidic acid (DPPA) complexes (Van Dijck et al., 1978; Liao and Prestegard, 1981; Graham et al., 1985; Kouaouci et al., 1985; Ohki et al., 1989; Laroche et al., 1991; Vincent and Levin, 1991). In contrast, the existence of phase transition for the $Ca^{2+}$-PA complex at acidic pH has been reported by several researchers (Boughriet et al., 1988; Vincent and Levin, 1991). Furthermore, Blume (1988, 1991) has reported that the DMPA at 1–2 mM concentration undergoes a phase transition at 61°C, even in the presence of equimolar $Ca^{2+}$.

These facts indicate that the phase behavior of the $Ca^{2+}$-PA complexes depends on the conditions or the sample preparations. In fact, two different results have been reported for the stoichiometry of the $Ca^{2+}$-PA complexes. A 1:1 binding has been suggested by many studies (Liao and Prestegard, 1981; Kouaouci et al., 1985; Laroche et al., 1991). On the other hand, Boughriet et al. (1988) have shown that one $Ca^{2+}$ binds to two DMPA molecules at pH 4. Furthermore, Blume (1991) has pointed out from analysis of titration calorimetry that not only 1:1 binding but also 2:1 binding occurs for $Ca^{2+}$-DMPA complexes. It has been reported that at neutral pH, calcium-PA complex forms cochleate lipid structure (Liao and Prestegard, 1981; Kouaouci et al., 1985), indicating spirally folded shells (Papahadjopoulos et al., 1976). However, the structure of

the Ca$^{2+}$-PA complex under acidic conditions is still unknown.

To make clear the difference in the Ca$^{2+}$-DMPA complexes under differing pH, we investigated the structural and thermotropic properties of the Ca$^{2+}$-DMPA complexes at acidic pH (pH 4) and neutral pH (pH 7.4), using static and temperature-scan x-ray diffraction and differential scanning calorimetry (DSC).

## MATERIALS AND METHODS

### Materials

A monosodium salt of dimyristoylphosphatidic acid (DMPA) was purchased from Sigma Chemical Co. (St. Louis, MO) and Nichiyu Liposome Co. (Tokyo, Japan), and was used without further purification. The lipids of both companies gave a single spot on a silica gel thin-layer plate developed with CHCl$_3$/CH$_3$OH/H$_2$O (65:25:4, by volume). Furthermore, the behavior of the phase transition of these lipids was examined using DSC. For a typical case, when a HEPES buffer (HEPES 50 mM, EDTA 1 mM, pH 7.3) was used, the transition temperatures were 49.6 ± 0.2°C and 49.8 ± 0.3°C, and the transition enthalpies were 5.7 ± 0.3 kcal/mol and 6.0 ± 0.3 kcal/mol, for Sigma's and Nichiyu's lipids, respectively. These values agree with the literature values at similar pH conditions (Blume, 1988, 1991; Blume and Tuchtenhagen, 1992). Calcium chloride and sodium hydroxide were purchased from Katayama Chemical Ltd. (Osaka, Japan).

### Sample preparation

The Ca$^{2+}$-DMPA complexes were obtained by adding calcium chloride solution to DMPA vesicle dispersion. The complex at acidic pH (pH 4) was prepared as follows. A chloroform solution of DMPA was placed in a small test tube. The solvent was evaporated under a nitrogen stream and then the sample was kept under reduced pressure overnight. The lipid was dispersed into pure water. The pH of this dispersion was about 7. The samples were heated to about 65°C (the transition temperature of DMPA at pH ~7 is about 50°C; Blume and Tuchtenhagen, 1992) for about 5 min and mechanically agitated while warm to get homogeneous dispersion. Calcium chloride solution was added to this DMPA vesicle dispersion. The volume and concentration of added CaCl$_2$ solution were equal to those of the DMPA dispersion, i.e., the number of Ca$^{2+}$ ions is equal to that of DMPA molecules. From this procedure, Ca$^{2+}$-DMPA complexes were formed. The complexes were heated above 80°C for 3 min with mechanical agitation and then cooled down to room temperature. Such cycles of heating and cooling were repeated at least three times to get a homogeneous sample. Addition of calcium ions induces the displacement of the protons on the surface of DMPA bilayers, and as a result the pH decreases. The pH of the supernatant fluid was about 4 after the complex formation. On the other hand, in the preparation of the complex at neutral pH (pH 7.4), DMPA molecules were dispersed into sodium hydroxide solution. The concentrations of NaOH solution were prepared so as to be equimolar to DMPA dispersion. Because monosodium-DMPA was used, there were two sodium ions for each DMPA molecule in this final dispersion. The pH of DMPA dispersion in the presence of NaOH was about 11. The samples were heated to about 50°C (the transition temperature of DMPA at pH ~11 is about 40°C; Blume and Tuchtenhagen, 1992) for about 5 min and mechanically agitated while warm. After the DMPA vesicles were formed, calcium chloride solution was added to form Ca$^{2+}$-DMPA complexes. The same cycles of heating and cooling were performed for the homogeneous complex formation. After the complex formation, the pH of supernatant fluid was about 7.4. It was confirmed by thin-layer chromatography that the cycles of heating and cooling for the complexes induce no degradation products. The lipid concentration was 100 mM for DSC measurements. For x-ray diffraction measurements, to obtain the sufficient intensities, we used a pellet of the sample that was precipitated by centrifugation.

## pH measurement

The pH measurements were performed with a Beckman 32 pH meter (Beckman Instruments, Inc., Fullerton, CA). A glass/calomel complex pH electrode (Beckman no. 39536) was used. Fifty microliters of the CaCl$_2$ solution (5 mM, pH 5.6) was added at a time to the DMPA dispersion (5 mM, 2 ml) or to the DMPA dispersion (5 mM, 2 ml), as was equimolar NaOH (5 mM). These measurements were performed at about 23°C.

## Inductively coupled plasma atomic emission spectrometry

The composition ratio of calcium atoms to phosphorus atoms for the complexes at acidic and neutral pH was measured directly using an inductively coupled plasma atomic emission spectrometer (ICP-AES). An ICP-AES system, SPS1500 (Seiko I and E, Japan), was operated under the following conditions: $R_f$ output power of 1.3 kW, carrier argon gas flow rate of 0.3 L/min, auxiliary gas flow rate of 0.5 L/min, outer gas flow rate of 15 L/min, and observation height of 15.1 mm above load coil. For the analyses, the lines were chosen at 213.618 nm for phosphorus and at 317.933 nm for calcium.

The samples for ICP-AES were prepared as follows. The precipitates (Ca$^{2+}$-DMPA complexes) were collected with a filter paper (no. 3, Advantec, Japan). The collected precipitates (about 10 mg) were dissolved into a mixture of sulfuric acid (0.5 ml) and nitric acid (3.0 ml) with heat to about 80°C on a hot plate. The samples were then diluted 25 times with water.

## Differential scanning calorimetry

Differential scanning calorimetric studies were performed with DSC10 and SSC580 (Seiko I and E, Japan) at a heating scan rate of 1.0°C/min. The calorimetric data were collected and stored automatically by a microcomputer using a data acquisition system provided by Seiko I and E. Transition enthalpies were evaluated by integrating the area under the transition curve. The scales for the both temperature and DSC thermogram were calibrated with a standard sample of gallium.

## X-ray diffraction

Static x-ray diffraction patterns were collected using an imaging plate (Type BAS-III, Fuji Photo Film Co., Ltd., Japan). A nickel filtered CuK$_\alpha$ x-ray beam produced by an RU-200BEH rotating anode generator (Rigaku, Tokyo, Japan) was collimated by double-mirror optics. The exposure times were 2–8 h. The sample cell was composed of an aluminum plate (1.0 mm in thickness) with a rectangular hole of 4 × 6 mm. The window of the sample cell was sealed by a pair of polyimide films. This sample cell was set on a water-jacketed sample holder. Temperature was kept constant by circulating water into the sample holder with a temperature-controlled water bath (Thermomix, B. Braun, Melsungen, Germany). The background caused by the scattering of water, the diffraction from a polyimide film, etc. were subtracted from each diffraction pattern. The pattern was averaged by azimuthally integrating two-dimensional Debye-Scherrer patterns (Takahashi et al., 1991).

Temperature-scan x-ray diffraction studies were performed at station 15A of the Photon Factory in National Laboratory for High Energy Physics (Tsukuba, Japan). The wavelength was 0.1504 nm. The optical system has been described by Amemiya et al. (1983) in detail. The photon flux was typically in the range of 2–8 × 10$^8$ photons/s. For each experiment, 92 diffraction patterns were collected consecutively using a one-dimensional position-sensitive proportional counter with 512 channels (PSPC, Rigaku, Tokyo, Japan) linked to the station computer. The exposure time for each

frame was 30 s. The sample holder and the method of temperature scan have been described in detail elsewhere (Tenchov et al., 1989).

The sample-to-detector distances for static and temperature-scan measurements were about 200 and 300 mm, respectively. The diffraction spacings were calibrated with a powder pattern of synthetic fluorophlogopite mica.

## Interpretation of lamellar reflection data

When the phase for each lamellar reflection is known, we can calculate a one-dimensional electron density profile along the bilayer normal from the data of intensity of lamellar reflection. There are several methods of phase determination. For lipid-water systems, a swelling method (Franks, 1976; Torbet and Wilkins, 1976) is a powerful one. However, the $Ca^{2+}$-DMPA complexes are unable to swell. Then we assumed a structural model for the $Ca^{2+}$-DMPA complexes, from which the structure factors for the lamellar reflections can be calculated. Using the following procedure, we searched for the fittest model from the comparison between the absolute values of calculated structure factors and the values of the structure factor obtained by experiments. In practice, we constructed a model including three adjustable parameters for the $Ca^{2+}$-DMPA complexes as follows. Fundamentally, the structure of the complex was assumed to be multilamellar. The position of the calcium ions along the bilayer normal direction is fixed at the central point between the neighboring DMPA bilayers. The position of the calcium ions was taken as the origin. The number of the calcium ions per DMPA molecule in the complexes was taken as one of the model parameters. The position of each atom of a lipid molecule was used in the atomic coordinate data of a sodium-DMPA crystal reported by Harlos et al. (1984). However, for the $Ca^{2+}$-DMPA complexes it was assumed that the hydrocarbon chains are untilted, because the lamellar spacing of the complexes is longer than that of the crystals. Therefore, to arrange the hydrocarbon chains to be untilted, the carbon atoms (C(22) and C(32)) in numbering by Harlos et al., 1984) that bind to the glycerol backbone were selected as the rotating center, and then each hydrocarbon chain was rotated (see Fig. 1). Because the atomic coordinates of hydrogen are not known for the DMPA crystal, the position of hydrogen atoms was assumed to be the same as that of the atoms to which the hydrogen atoms were bound.

The calculated structure factor $(F_c(h))$ for the molecular model of the $Ca^{2+}$-DMPA complex is represented by

$$F_c(h) = \sum_j u_j \cdot f_j \cdot \exp\{2\pi i(h \cdot x_j)\}, \qquad (1)$$

$$u_j = \exp\{8\pi i(h \cdot x_j)^2 \cdot (\sin \theta/\lambda)^2\}, \qquad (2)$$

where $j$ denotes each atom, $f_j$ is the atomic form factor, $u_j$ is the thermal displacement, $\theta$ is the scattering angle, $\lambda$ is the wavelength of x-ray, $h$ is the order of refection, and $x_j$ is the coordinate of the $j$ atom. For the atomic form factor of each atom, an analytical representation (Sakurai, 1967) was used. This representation is expressed by the sum of two Gaussian shape functions (Vand et al., 1957; Forsyth and Wells, 1959). For all atoms in the $Ca^{2+}$-DMPA complex, the thermal displacement $(u_j)$ is assumed to have the same value $(u)$. Our model has three parameters: 1) The position of the phosphorus atom of the DMPA $(X(P)$ (nm)), where the origin was taken at the position of the calcium ions; 2) the mean thermal displacement $(u$ (nm)). 3) The number of calcium ions per DMPA molecule (Ca/DMPA). The optimal values of these three parameters were determined by searching the minimum of the residue $R$ defined by

$$R = \frac{\sum ||F_c(h)| - K|F_o(h)||}{\sum K|F_o(h)|}, \qquad (3)$$

where $K$ is a scaling factor defined by

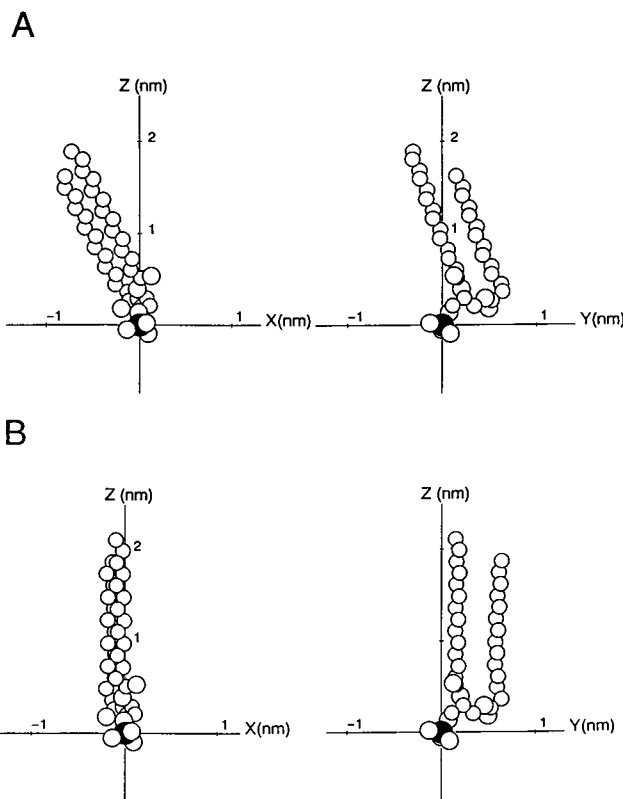$$K = \frac{\sum |F_c(h)|}{\sum |F_o(h)|}, \qquad (4)$$



FIGURE 1 (A) Projection of molecular conformation of DMPA in a crystal (Harlos et al., 1984) onto the b-c plane (left) and a-c plane (right). (B) Projection of molecular conformation of DMPA in a model used for analysis in this study onto the b-c plane (left) and a-c plane (right). The phosphorus atom was placed at the origin.

where $|F_o(h)|$ is the absolute value of the observed normalized structure factor. This value is the square root of the integrated intensity and is normalized as $|F_o(1)| = 1.00$. We used the minimization program developed by Okumura (1986). The program is constructed based upon a simplex algorithm (Nelder and Mead, 1965). The data analysis was performed on a personal computer (PC-9801RX, NEC, Tokyo, Japan).

## RESULTS AND DISCUSSION

### Stoichiometry of Ca²⁺-DMPA complex

*pH change of DMPA dispersion by adding Ca²⁺*

For the DMPA dispersion (5 mM, 2 ml) in the presence of NaOH (5 mM), the pH was $10.8 \pm 0.2$. The binding of $Ca^{2+}$ to the DMPA bilayer induces the dissociation of the protons on the membrane surface. As a result, the pH decreases (Fig. 2). When the value of the $Ca^{2+}$/DMPA ratio is greater than 1.0, the pH is almost constant (pH $\sim$7). On the other hand, the pH was $7.5 \pm 0.1$ for the DMPA dispersion in pure water without NaOH. The pH of pure water used in this study was about 5.5. Because the surface negative charge of vesicles attracts protons, the pH becomes higher (Träuble et al., 1976). When the $Ca^{2+}$/DMPA ratio is greater than 0.5, the pH is almost constant (pH $\sim$4). These results indicate that the stoichiometry between DMPA and $Ca^{2+}$
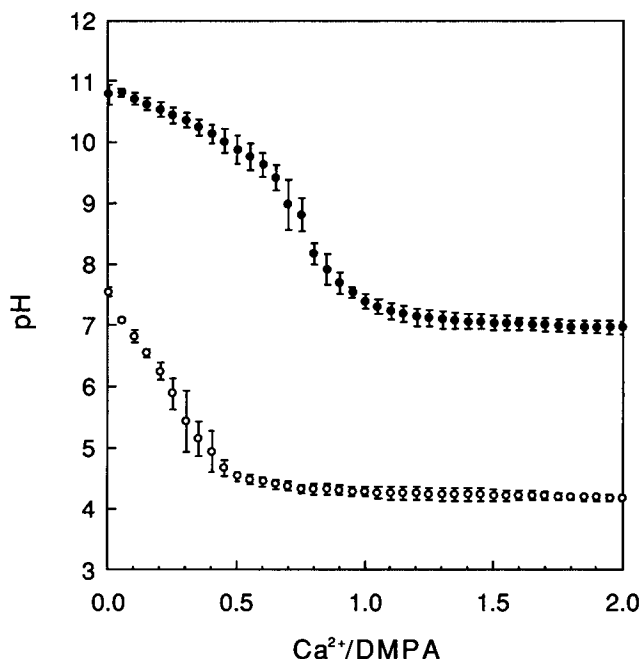
FIGURE 2  pH variations versus $Ca^{2+}$/DMPA molar ratio. Closed circles indicate the case of adding $Ca^{2+}$ to DMPA dispersion (5 mM) in the presence of equimolar NaOH (5 mM). Open circles indicate the case of adding $Ca^{2+}$ to DMPA dispersion (5 mM) in pure water.

## Structural characteristics of Ca²⁺-DMPA complexes

### Static x-ray diffraction measurements

The diffraction patterns for the $Ca^{2+}$-DMPA complexes at pH 7.4 and 4 at 20°C are displayed in Fig. 3, $A$ and $B$, respectively. Sharp lamellar reflections indicate that $Ca^{2+}$-DMPA complexes at pH 7.4 and 4 form highly ordered multilamellar structures. The diffraction profiles in the wide-angle region (around $S = 2.5$ nm⁻¹) were different between the complexes at pH 7.4 and 4. The $Ca^{2+}$-DMPA complex at pH 7.4 gives rise to only one reflection for the chain packing at 0.414 nm (Fig. 3 $A$). In contrast, two peaks appear at 0.413 nm and 0.381 nm for the complex at pH 4 (Fig. 3 $B$). The former result implies that the hydrocarbon chains of the $Ca^{2+}$-DMPA complex at pH 7.4 are packed in a hexagonal lattice. The latter result implies that the hydrocarbon chains of the complex at pH 4 are packed in an orthorhombic lattice in which the lattice spacings of d(11) and d(1-1) are 0.413 nm and d(20) is 0.381 nm. The same fact has been suggested from the studies of Raman spectroscopy (Vincent and Levin, 1991) for the $Ca^{2+}$-DMPA complex at acidic pH. The occupied area per hydrocarbon chain calculated from the observed spacings at pH 4 (0.187 nm²) is smaller than the area at pH 7.4 (0.198 nm²). Therefore, the hydrocarbon chains of the complex at pH 4 are
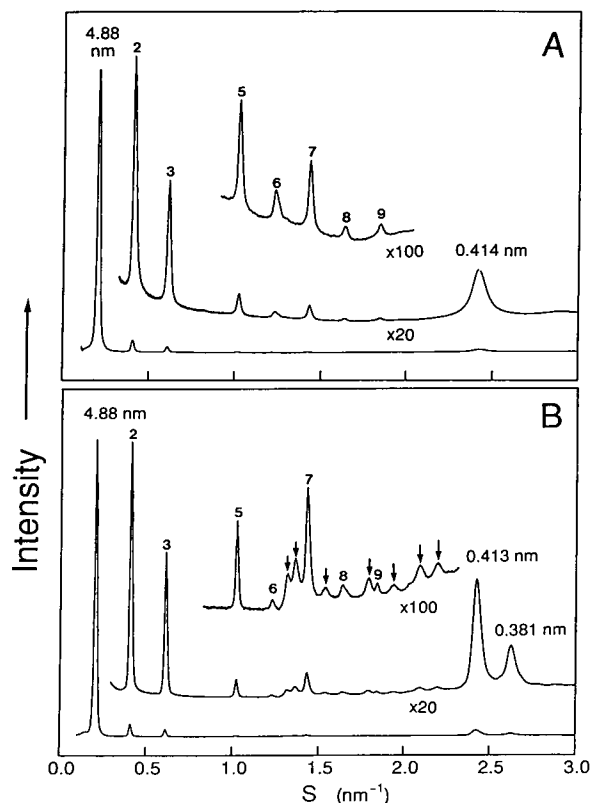
depends on the conditions of the DMPA dispersion before adding $Ca^{2+}$. In the presence of NaOH (pH ~11), the stoichiometry is one DMPA molecule per $Ca^{2+}$ ion. This result agrees with the previously reported results (Liao and Prestegard, 1981; Bicknell-Brown et al., 1986; Laroche et al., 1991). In contrast, in the case of the addition of only $Ca^{2+}$ ions to a DMPA bilayer, the stoichiometry is two lipid molecules per $Ca^{2+}$ ion. Boughriet et al. (1988) have reported an identical result for $Ca^{2+}$-DMPA complex at pH 4.

The dissociation of the second proton of DMPA is induced by the addition of NaOH (Blume and Tuchtenhagen; 1992), i.e., $DMPA^-$ changes to $DMPA^{2-}$ in the presence of NaOH. Therefore, one $DMPA^{2-}$ binds to one $Ca^{2+}$ for the case of the starting DMPA dispersion containing NaOH (pH ~11).

## ICP-AES measurements

For three samples of the $Ca^{2+}$-DMPA complexes at acidic pH and neutral pH, amounts of P and Ca were measured using ICP-AES. The ratio of $Ca^{2+}$ to DMPA was 1.00 ± 0.07 for the complex at neutral pH. On the other hand, for the complex at acidic pH, the ratio of $Ca^{2+}$ ions to DMPA molecules was 0.67 ± 0.02. The latter value is slightly larger than that determined by the pH measurements. However, they are essentially consistent.



FIGURE 3  Static x-ray diffraction patterns for $Ca^{2+}$-DMPA complex at pH 7.4 ($A$) and pH 4 ($B$) at 20°C. $S$ is defined as 2 sin $\theta/\lambda$, where $2\theta$ is the scattering angle and $\lambda$ is the wavelength of x-ray.

more tightly packed than those at pH 7.4. It is worthwhile to point out that the area at pH 4 is almost the same as the area of a crystal of monosodium-DMPA (0.186 $nm^2$) (Harlos et al., 1984). Thus, the packing of the hydrocarbon chains at pH 4 is similar to that of the crystal, i.e., the complex at pH 4 is crystalline-like in this sense.

A most remarkable feature for the diffraction pattern of the $Ca^{2+}$-DMPA complex at pH 4 is that several reflections were observed in the range of $S = 1.2$–$2.4$ $nm^{-1}$. These reflections do not correspond to the higher orders of the lamellar reflections. This fact also indicates that the $Ca^{2+}$-DMPA complex at pH 4 is more ordered than the complex at pH 7.4. Such observations have been made for dipalmitoylphosphatidylcholine (Füldner, 1981; Ruocco and Shipley, 1982a) or dipalmitoylphosphatidylglycerol (Wilkinson and McIntosh, 1986; Blaurock and McIntosh, 1986; Takahashi et al., 1992) in the subgel phase, metal ion-phosphatidylserine complexes (Hauser and Shipley, 1981, 1984), and fully hydrated dilauroylphosphatidyleth-anolamine in the highly ordered phase (Chang and Epand; 1983; Seddon et al., 1983), etc. These reflections suggest that there is a characteristic lattice that may be related to the arrangement of the $Ca^{2+}$ ions. However, on the basis of the limited information for the unoriented samples, the indices of the new reflections could not be determined unambiguously.

The electron density profiles for the $Ca^{2+}$-DMPA complexes at pH 7.4 and 4 are shown in Fig. 4, A and B, respectively, with the profiles calculated in the same resolution from the models with the best-fit parameters. The best-fit parameters are summarized in Table 1, where the phase angles were $\pi$ for the all of the reflections in both complexes. The R-factors for the complexes at pH 4 and 7.4 were 0.11 and 0.07, respectively. For the both profiles, the highest density peaks at the origin correspond to the position of the $Ca^{2+}$ ions and the second highest peaks at both sides of this highest peak correspond to the DMPA head-groups. The lowest electron density trough near $\pm 2.5$ nm corresponds to the gap between the terminal methyl groups of the lipid hydrocarbon chains. These electron density profiles imply that the $Ca^{2+}$ ions distribute in the narrow region and that the ions bridge between the adjacent bilayers. However, the clear difference between the complexes at pH 4 and 7.4 could not be found at the electron densities of the $Ca^{2+}$ ion region. For the number of $Ca^{2+}$ ions per lipid molecule, they are estimated to be almost the same (1.2–1.3). In the above analyses, we assumed that the electron density around the origin was generated only from $Ca^{2+}$ ions. However, these results suggest the existence of substances between the DMPA bilayers in addition to the $Ca^{2+}$ ion. In fact, Laroche et al. (1991) have proposed the existence of binding water molecules in the $Ca^{2+}$-DMPA complex at neutral pH.

Static x-ray diffraction measurements were also performed at various temperatures. The $Ca^{2+}$-DMPA complex at pH 7.4 does not undergo the chain melting up to 80°C (Fig. 5 A). This result is consistent with the observation by
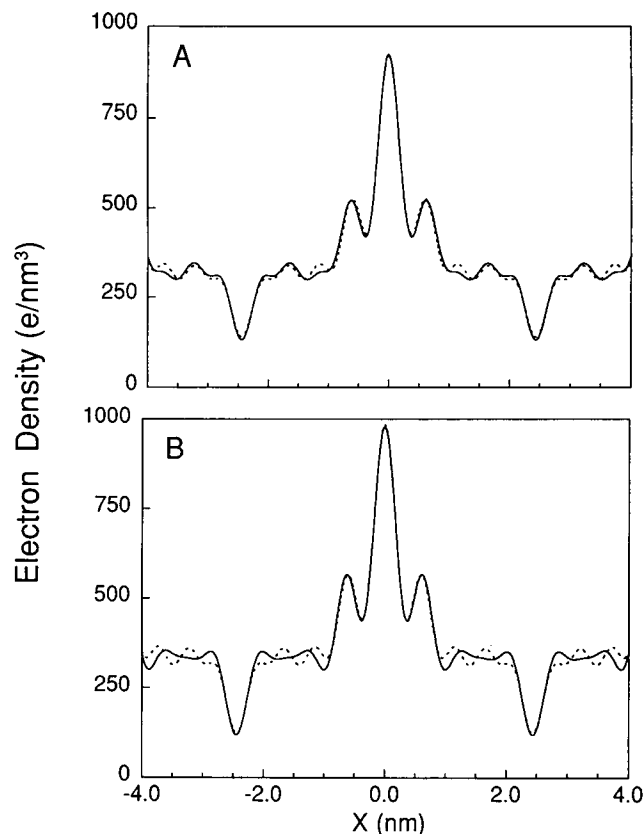


FIGURE 4   Electron density profiles for $Ca^{2+}$-DMPA complex at (A) pH 7.4 and (B) pH 4 at 20°C. The model electron density profiles calculated with the same resolution (dash line) are also displayed.

Laroche et al. (1991). On the other hand, the structural change was observed for the complex at pH 4 (Fig. 5 B). The broad scattering pattern in the wide-angle region at 80°C indicates chain melting. Two kinds of reflection were

**TABLE 1   The parameters at the best fitting for the $Ca^{2+}$-DMPA complexes at pH 7.4 and pH 4 and a comparison between the experimental ($KF_o$) and the calculated ($F_c$) structure factors in the observed orders of the diffractions**

|  | pH 7.4 | | pH 4 | |
|---|---|---|---|---|
| $X(P)$ (nm) | 0.53 | | 0.50 | |
| $u$ (nm) | 0.10 | | 0.08 | |
| Ca/DMPA | 1.3 | | 1.2 | |
| R-factor | 0.07 | | 0.11 | |
| $h$ | $K\|F_o\|$ | $F_c$ | $K\|F_o\|$ | $F_c$ |
| 0 | — | 750 | — | 743 |
| 1 | 169 | 157 | 167 | 172 |
| 2 | 65 | 65 | 67 | 61 |
| 3 | 72 | 71 | 76 | 76 |
| 4 | 0 | 7 | 0 | 3 |
| 5 | 49 | 45 | 44 | 46 |
| 6 | 38 | 31 | 23 | 29 |
| 7 | 58 | 53 | 74 | 57 |
| 8 | 31 | 37 | 38 | 40 |
| 9 | 34 | 38 | 30 | 43 |

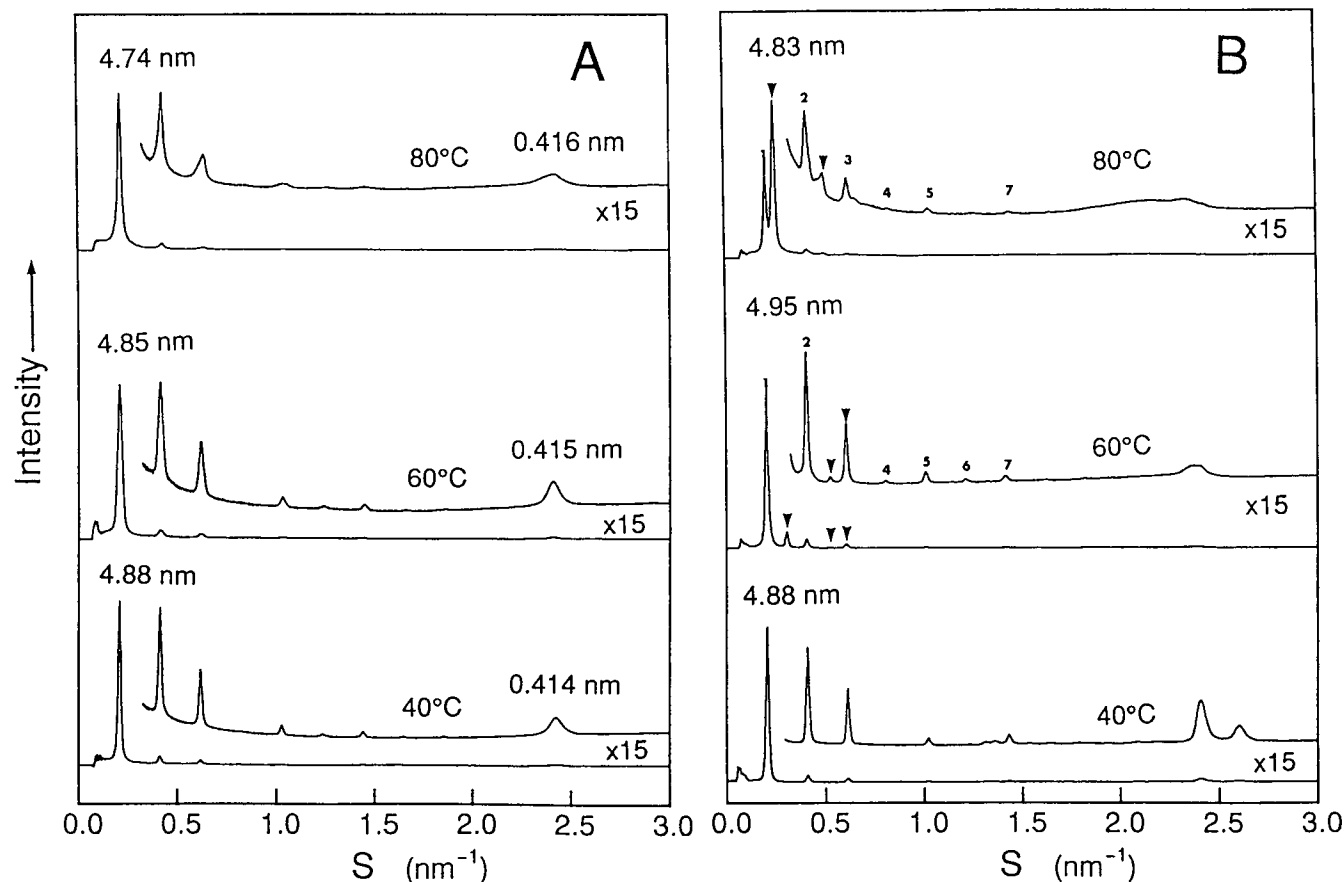The notations, $X(P)$, $u$, Ca/DMPA, and R-factor are described in the text.

FIGURE 5   Static x-ray diffraction patterns for Ca²⁺-DMPA complex at pH 7.4 (*A*) and pH 4 (*B*) at 40, 60, and 80°C.

observed in the small-angle region at 60°C. The reflections denoted by numbers 1 to 7 in Fig. 5 *B* correspond to the lamellar structure. In addition to these reflections, we observed the reflections denoted by arrowheads with the spacing of 3.30, 1.90, and 1.65 nm. The ratio of the spacings is $1:1/\sqrt{3}:1/2$. This fact indicates the formation of a hexagonal II structure. Boughriet et al. (1988) have observed that the hexagonal II structure appears for the Ca²⁺-DPPA complex (2:1 molar ratio) above 75°C. Two different lamellar reflections were also observed at 80°C. The longer lamellar spacing is 4.83 nm, and the shorter one (denoted by arrowheads in the profile at 80°C in Fig. 5 *B*) is 4.01 nm. In fact, the structure of the Ca²⁺-DMPA complex at pH 4 at higher temperatures (>60°C) is complicated; that is, two structures may coexist or an additional intermediate structure may be formed, as in the case of the Ca²⁺-dioleoylphospahtidic acid complex at pH > 5.0 (Farren et al., 1983).

## Thermotropic behavior of Ca²⁺-DMPA complexes

### DSC measurements

Fig. 6, *A* and *B*, shows the DSC thermograms of the Ca²⁺-DMPA complexes at pH 7.4 and 4, respectively. For the case of pH 4, the thermogram of the second heating scan
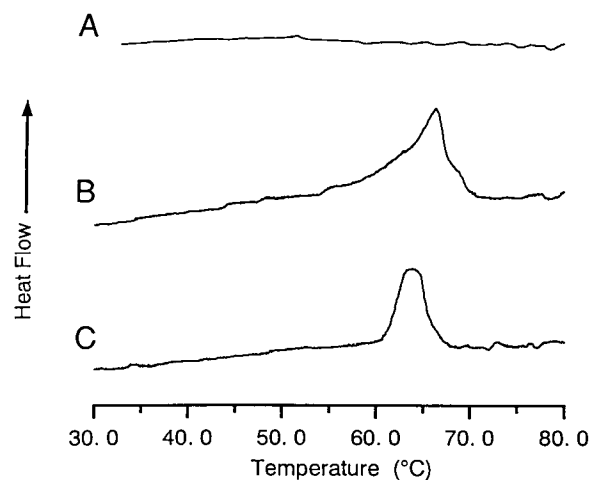


FIGURE 6   DSC thermograms for (*A*) Ca²⁺-DMPA complex at pH 7.4 and (*B* and *C*) Ca²⁺-DMPA at pH 4. For *C*, the measurements were performed in the second heating scan without incubation after rapid cooling from 80°C. The scanning rate in all of the measurements was 1.0°C/min.

after rapid cooling (> 1.0°C/min) is also shown (Fig. 6 *C*). The heating scan rate was 1.0°C/min. No phase transition peak was observed for the complex at pH 7.4 in the mea-

sured temperature range. The same result has been reported using various methods (Liao and Prestegard, 1981; Graham et al., 1985; Kouaouci et al., 1985; Laroche et al., 1991). On the other hand, a transition peak was observed in the DSC curve of the Ca$^{2+}$-DMPA complex at pH 4 in the first scan after incubation at 4°C for several days (Fig. 6 B). The peak temperature lies at 65.8 ± 0.8°C. The thermogram of the complex at pH 4 in the second scan exhibits rather sharper transition than that of the first scan (Fig. 6, B and C). The peak temperature (63.5 ± 1.5°C) is lower than that of the first scan. The transition enthalpy of the first scan (9.7 ± 2.1 kcal/mol) is greater than that of the second scan (4.1 ± 1.7 kcal/mol). The thermogram for the Ca$^{2+}$-DMPA at pH 4 incubated at a room temperature (23–25°C) for 4 days was similar to that of the first scan (data not shown). These facts suggest that there is a metastable state for the Ca$^{2+}$-DMPA complex at pH 4, i.e., after the rapid cooling from above the transition temperature, the complex at pH 4 forms to a metastable state and then the complex gradually converts to a stable phase after a long incubation at a temperature lower than room temperature.

## Temperature-scan x-ray diffraction measurements for complex at pH 4

Temperature-scan wide-angle x-ray diffraction measurements were performed for the Ca$^{2+}$-DMPA complex at pH 4 with the same scan rate (1.0°C/min) as the DSC study in the previous section. In the first heating scan after incubation at 4°C for several days, the diffraction profile shows complicated behavior (Fig. 7 A). First, the two peaks (0.413 nm and 0.382 nm at 40°C) appear. Second, when the tem-

perature reaches about 52°C, the third sharp peak appears at the small-angle side of the two peaks and the intensities of two peaks decrease. Near 65°C, the intensity of the third peak decreases and then, the peak disappears at about 67°C. During the second scan after rapid cooling from above the phase transition temperature, a single peak that is indicative of hexagonal lattice packing appears, and when the temperature reaches about 63°C, the intensity of the peak decreases as a result of chain melting (Fig. 7 B). These results agree with the DSC measurements. The spacings of the peaks at about 0.41 nm and 0.38 nm are almost constant against temperature change (Fig. 7 C). On the other hand, the spacing of the peak in the 0.42–0.43 nm region gradually increases as the temperature rises for both the first and the second scans. Furthermore, as seen in the upper plots of Fig. 7 C, these peaks for the first and the second scans trace the same value of the spacing, i.e., they show the same temperature dependence. These results indicate that the hydrocarbon chains are packed in the same hexagonal lattice for both the first and the second scans. However, the temperatures of the chain melting are slightly different for the two scans. From the result of Raman spectroscopy of the Ca$^{2+}$-DMPA complex at pH 4 (Vincent and Levin, 1991), two different phase transitions have been reported. The authors have concluded that in the heating process, the lateral packing of the lipid molecules expands at the first step and the hydrocarbon chains melt at the second step. As seen in Fig. 7 A, the present results show that the expansion of the lateral packing of the lipid molecules results from the rearrangement of hydrocarbon chain packing from an orthorhombic to a hexagonal lattice.
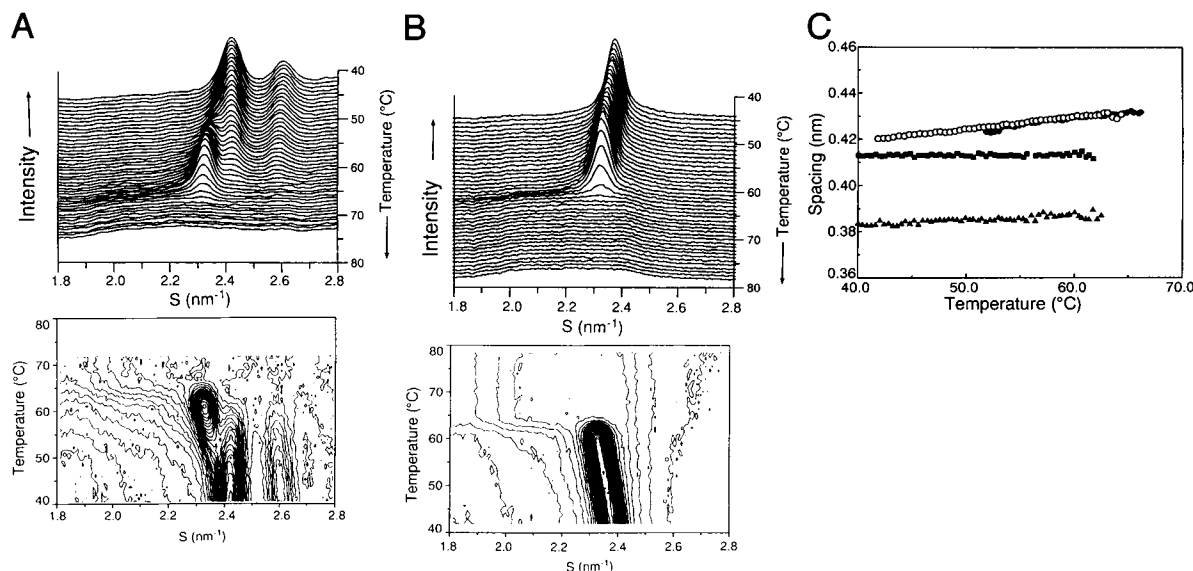


FIGURE 7 Temperature-scan x-ray diffraction patterns for Ca$^{2+}$-DMPA complex at pH 4 in (A) the first heating scan and (B) the second heating scan without incubation after rapid cooling from 80°C. The figures at the bottom represent the contour plots of the relative heights of the intensities. The highest intensity was divided into 20 height levels. (C) The observed spacings as a function of temperature. Closed marks correspond to the first scan. Open circles correspond to the second scan. The scanning rate of the all experiments was 1.0°C/min.

## Transformation of x-ray diffraction patterns of complex at pH 4 after rapid cooling

The time course of the gel to subgel phase transformation in dipalmitoylphosphatidylcholine has been studied intensively by x-ray diffraction (Ruocco and Shipley, 1982b; Akiyama, 1985; Akiyama et al., 1987; Tristram-Nagle et al., 1994). A series of x-ray diffraction patterns was observed at 20°C for the $Ca^{2+}$-DMPA complex at pH 4 at various times after rapid cooling from 80 to 20°C, as seen in Fig. 8. The lamellar spacing of the $Ca^{2+}$-DMPA complex at pH 4 is 5.18 nm immediately after rapid cooling. The packing of the hydrocarbon chains is also different from that of the stable crystalline-like phase. The lattice spacing of the chain is 0.411 nm. The appearance of only one sharp peak is indicative of hexagonal lattice packing. No reflection in the range of $S = 0.9$–$2.4$ $nm^{-1}$ suggests that the complex after rapid cooling is more disordered than that in the stable phase. In the pattern obtained 16–19 h after cooling, two kinds of lamellar spacings were observed. One spacing corresponds to the meta-stable state and the other corresponds to the stable phase. The reflection belonging to the metastable state was not detected in the pattern obtained 60–65 h after cooling. The profile obtained 86–93 h after rapid cooling is identical with that of the stable phase. This experiment shows that the $Ca^{2+}$-DMPA complex at pH 4 slowly (in about 90 h) converts from the metastable state to the stable state by incubation at a temperature lower than room temperature. This phenomenon might be strongly related to the formation of the subgel phase of phosphatidylcholines (Chen et al., 1980; Lewis et al., 1987, 1988) or phosphatidylglycerols (Wilkinson and McIntosh, 1986; Epand et al., 1992; Kodama et al., 1993) during the long incubation at low temperature.

## CONCLUSIONS

The experimental results presented in this paper lead us to the following conclusions: 1) The nature of the $Ca^{2+}$-DMPA complexes formed depends on the conditions of the starting dispersion. 2) The stoichiometries of $Ca^{2+}$ ion to DMPA molecule are 0.5–0.67 and ~1 for the complexes at pH 4 and 7.4, respectively. 3) The complex at pH 4 at 20°C is more ordered than the complex at pH 7.4 at 20°C, i.e., the former has a crystalline-like structure in which the hydrocarbon chains are packed tightly in an orthorhombic lattice. 4) The $Ca^{2+}$-DMPA complex at pH 4 undergoes two phase transitions in contrast to no phase transition for the complex at pH 7.4. For the $Ca^{2+}$-DMPA complex at pH 4 the lower phase transition occurs at ~ 52°C. At this phase transition, the lattice of the hydrocarbon chain changes from an orthorhombic to a hexagonal lattice. Subsequently, the chain melting phase transition occurs at ~ 67°C. 5) After rapid cooling from a temperature higher than the chain melting transition temperature to room temperature, the $Ca^{2+}$-DMPA complex at pH 4 takes on a metastable state.

FIGURE 8   Time variation of static x-ray diffraction patterns for the $Ca^{2+}$-DMPA complex at pH 4 at 20°C after rapid cooling from 80°C. The numerals indicate time in hours after cooling.

## REFERENCES

Akiyama, M. 1985. X-ray diffraction studies of subtransition in dipalmitoylphosphatidylcholine. *Jpn. J. Appl. Phys.* 24:231–234

Akiyama, M., N. Matsushima, and Y. Terayama. 1987. Kinetics of the subtransition of multilamellar dipalmitoylphosphatidylcholine. *Jpn. J. Appl. Phys.* 26:1587–1591

Amemiya, A., K. Wakabayashi, T. Hamanaka, T. Wakabayashi, T. Matsushita, and H. Hashizume. 1983. Design of a small-angle x-ray diffractomer using synchrotron radiation at the photon factory. *Nucl. Instrum. Methods.* 208:471–477.

Bicknell-Brown, E., K. G. Brown, and D. Borchman. 1986. Atomic and Raman spectroscopy of dipalmitoylphosphatidic acid-calcium complex and phase transition. *Biochim. Biophys. Acta.* 862:134–140

Blume, A. 1988. Application of calorimetry to lipid model membranes. *In* Physical Properties of Biological Membranes and Their Function Implications. C. Hidalgo, editor. Plenum, New York. 71–121.

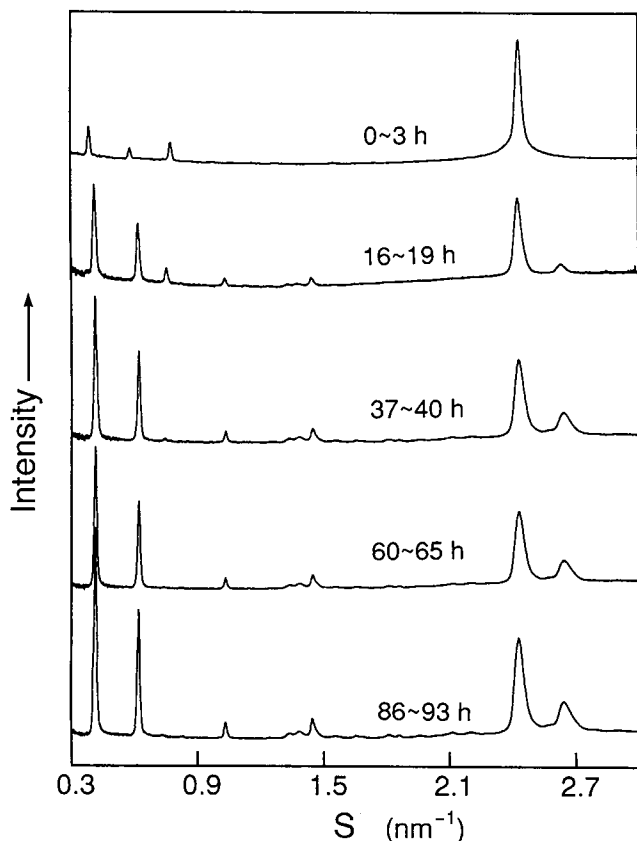Blume, A. 1991. Biological calorimetry: membranes. *Thermochim. Acta.* 193:299–357

Blume, A., and J. Tuchtenhagen. 1992. Thermodynamic of ion binding to phosphatidic acid bilayers. Titration calorimetry of the heat of dissociation of DMPA. *Biochemistry.* 31:4636–4642.

Boughriet, A., M. Ladajadj, and E. Bicknell-Brown. 1988. Calcium-induced condensation-reorganization phenomena in multilamellar vesicles of phosphatidic acid. pH potentiometric and $^{31}$P-NMR, Raman and ESR spectroscopic studies. *Biochim. Biophys. Acta.* 939:523–532.

Caffrey, M., and G. W. Feigenson. 1984. Influence of metal ions on the phase properties of phosphatidic acid in combination with natural and synthetic phosphatidylcholines: an x-ray diffraction study using synchrotron radiation. *Biochemistry.* 23:323–331.

Chang, H., and R. M. Epand. 1983. The existence of a highly ordered phase in fully hydrated dilauroylphosphatidylethanolamine. *Biochim. Biophys. Acta.* 728:319–324.

Chen, S. C., J. M. Sturtevant, and B. J. Gaffney. 1980. Scanning calorimetric evidence for a third phase transition in phosphatidylcholine bilayers. *Proc. Natl. Sci. USA.* 77:5060–5063.

Dennis, E. A., S. G. Rhee, M. M. Billah, and Y. A. Hannun. 1991. Role of phosholipases in generating lipid second messengers in siganal transduction. *FASEB J.* 5:2068–2077.

Eklund, K. K., J. Vurorinen, J. Mikkola, J. A. Viranen, and P. K. J. Kinnunen. 1988. Ca$^{2+}$-induced lateral phase separation in phosphatidic acid/phosphatidylcholine monolayers as revealed by fluorescence microscopy. *Biochemistry.* 27:3433–3437.

Epand, R. M., B. Gabel, R. F. Epand, A. Sen, S. W. Hui, A. Muga, and W. K. Surewicz. 1992. Formation of a new stable phase of phosphatidylglycerols. *Biophys. J.* 63:327–332.

Farren, S. B., M. J. Hope, and P. R. Cullis. 1983. Polymorphic phase preferences of phosphatidic acid: A $^{31}$P and $^2$H NMR study. *Biochem. Biophys. Res. Commun.* 111:675–682.

Forsyth, J. B., and M. Wells. 1959. On an analytic approximation to the atomic scattering factor. *Acta Cryst.* 12:412–415.

Franks, N. P. 1976. Structural analysis of hydrated egg lecithin and cholesterol bilayers. I. X-ray diffraction. *J. Mol. Biol.* 100:345–358.

Füldner, H. H. 1981. Characterization of a third phase transition in multilamellar dipalmitoylphosphatidylcholine liposomes. *Biochemistry.* 20: 5707–5710.

Graham, I., J. Gagné, and J. R. Silvius. 1985. Kinetics and thermodynamics of calcium-induced lateral phase separations in phosphatidic acid containing bilayers. *Biochemistry.* 24:7123–7131.

Harlos, K., H. Eibl, I. Pacher, and S. Sundell. 1984. Conformation and packing properties of phosphatidic acid: the crystal structure of monosodium dimyristoylphosphatididate. *Chem. Phys. Lipids.* 34:115–126.

Hauser, H., and G. G. Shipley. 1981. Crystallization of phosphatidylserine bilayers induced by lithium. *J. Biol. Chem.* 25:11377–11380.

Hauser, H., and G. G. Shipley. 1984. Interaction of divalent cations with phosphatidylserine bilayer membranes. *Biochemistry.* 23:34–41.

Kodama, M., T. Miyama, and T. Yokoyama. 1993. Crystalline cylindrical structures of Na$^+$-bound dimyristoylphosphatidylglycerol as revealed by microcalorimetry and electron microscopy. *Biochim. Biophys. Acta.* 1168:243–248.

Kouaouci, R., J. R. Silvius, I. Graham, and M. Pézolet. 1985. Calcium-induced lateral phase separation in phosphatidylcholine-phosphatidic acid mixtures. A Raman spectroscopic study. *Biochemistry.* 24: 7132–7140.

Laroche, G., E. J. Dufourc, J. Dufourcq, and M. Pézolet. 1991. Structure and dynamics of dimyristoylphosphatidic acid/calcium complexes by $^2$H NMR, infrared, and Raman spectroscopies and small-angle x-ray diffraction. *Biochemistry.* 30:3105–3114.

Lewis, R. N. A., N. Mak, and R. N. McElhaney. 1987. A differential scanning calorimetric study of the thermotropic phase behavior of model membranes composed of phosphatidylcholines containing linear saturated fatty acyl chains. *Biochemistry.* 26:6118–6126.

Lewis, R. N. A., B. D. Sykes, and R. N. McElhaney. 1988. Thermotropic phase behavior of model membranes composed of phosphatidylcholines containing cis-monounsaturated fatty acyl chain homologues of oleic acid: differential scanning calorimetric and $^{31}$P NMR spectroscopic studies. *Biochemistry.* 27:880–887.

Liao, M. J., and J. H. Prestegard. 1981. Structural properties of a Ca$^{2+}$-phosphatidic acid complex: small angle x-ray scattering and calorimetric results. *Biochim. Biophys. Acta.* 645:149–156.

Nelder, J. A., and R. Meade. 1965. A simplex method for function minimization. *Comput. J.* 7:308–313.

Nishizuka, Y. 1992. Intracellular signaling by hydrolysis of phospholipids and activation of protein kinase C. *Science.* 258:607–614.

Ohki, K. 1988. Ca$^{2+}$-induced lateral phase separation in ternary mixtures of phosphatidic acid, phosphatidylcholine, and phosphatidylethanolamine inferred by calorimetry. *J. Biochem.* 104:14–17.

Okhi, K., S. Nagaoka, M. Sogami, and Y. Nozawa. 1986. Ca$^{2+}$-translocation activities of phosphatidylinositol, diacylglycerol and phosphatidic acid inferred by quin-2 in artificial membrane systems. *Chem. Phys. Lipids.* 39:237–249.

Ohki, K., K. Takahashi, S. Kato, and A. Maesono. 1989. Short- and long-range Ca$^{2+}$-induced lateral phase separation in ternary mixture of phosphatidic acid, phosphatidylcholine and phosphatidylethanolamine. *Chem. Phys. Lipids.* 50:109–177.

Okumura, H. 1986. Introduction to Data Analysis by Personal Computer. (in Japanese) Gijitsu Hyoron-sha, Tokyo.

Papahadjopoulos, D., W. J. Vail, W. A. Pangborn, and G. Poste. 1976. Studies on membrane fusion: induction of fusion in pure phospholipid membranes by calcium ions and other divalent metals. *Biochim. Biophys. Acta.* 448:265–283.

Ruocco, M. J., and G. G. Shipley. 1982a. Characterization of the subtransition of hydrated dipalmitoylphosphatidylcholine bilayers: x-ray diffraction study. *Biochim. Biophys. Acta.* 684:59–66.

Ruocco, M. J., and G. G. Shipley. 1982b. Characterization of the subtransition of hydrated dipalmitoylphosphatidylcholine bilayers: kinetic, hydration and structural study. *Biochim. Biophys. Acta.* 691:309–320.

Sakurai, T. 1967. X-ray Analysis of Crystal Structure. (in Japanese) Shoukabo, Tokyo.

Seddon, J. M., K. Harlos, and D. Marsh. 1983. Metastability and polymorphism in the gel and fluid bilayer phases of dilauroylphosphatidylethanolameine. Two crystalline forms in excess water. *J. Biol. Chem.* 25:3850–3854.

Smaal, E. B., J. G. Mandersloot, R. A. Demel, B. de Kruijff, and J. de Gier. 1987. Consequences of the interaction of calcium with dioleoylphosphatidate-containing model membranes: calcium-membrane and membrane-membrane interactions. *Biochim. Biophys. Acta.* 897:180–190.

Takahashi, H., S. Matuoka, S. Kato, K. Ohki, and I. Hatta. 1991. Electrostatic interaction of poly(L-lysine) with dipalmitoylphosphatidic acid studied by x-ray diffraction. *Biochim. Biophys. Acta.* 1069:229–234.

Takahashi, H., S. Matuoka, S. Kato, K. Ohki, and I. Hatta. 1992. Effects of poly(L-lysine) on the structural and thermotropic properties of dipalmitoylphoshatidylglycerol bilayers. *Biochim. Biophys. Acta.* 1110:29–36.

Tenchov, B. G., H. Yao, and I. Hatta. 1989. Time-resolved x-ray diffraction, and calorimetric studies at low scan rates. I. Fully hydrated dipalmitoylphosphatidylcholine (DPPC), and DPPC/water/ethanol phases. *Biophys. J.* 56:757–768.

Torbet, J., and M. H. F. Wilkins. 1976. X-ray diffraction studies of lecithin bilayers. *J. Theor. Biol.* 62:447–458.

Träuble, H., M. Teubner, P. Woolley, and H. Eibl. 1976. Electrostatic interactions at charged lipid membranes. I. Effects of pH and univalent cations on membrane structure. *Biophys. Chem.* 4:319–342.

Tristram-Nagle, S., R. M. Suter, W.-J. Sun, and J. F. Nagle. 1994. Kinetics of subgel formation in DPPC: x-ray diffraction proves nucleation-growth hypothesis. *Biochim. Biophys. Acta.* 1191:14–20.

Vand, V., P. F. Eiland, and R. Pepinsky. 1957. Analytical representation of atomic scattering factors. *Acta Crystallogr.* 10:303–306.

Van Dijck, P. W. M., B. de Kruijff, A. J. Verkleij, L. L. M. Van Deenen, and J. de Gier. 1978. Comparative studies on the effects of pH and Ca$^{2+}$ on bilayers of various negatively charged phospholipids and their mixtures with phosphatidylcholine. *Biochim. Biophys. Acta.* 512:84–96.

Vincent, J. S., and I. W. Levin. 1991. Raman spectroscopic studies of dimyristoylphosphatidic acid and its interaction with ferricytochrome c in cationic binary and ternary lipid-protein complexes. *Biophys. J.* 59: 1007–1021.

Wilkinson, D. A., and T. J. McIntosh. 1986. A subtransition in a phospholipid with a net charge, dipalmitoylphosphatidylglycerol. *Biochemistry.* 25:295–298.